



## Research Article

# FABRICATION AND STUDY OF RELEASE KINETICS OF MOXIFLOXACIN AND DEXAMETHASONE LOADED NANOSTRUCTURED LIPID CARRIER SYSTEM FOR OCULAR DRUG DELIVERY

Narayan Hemnani, Preeti K. Suresh\*

### Article Information

Received: 18<sup>th</sup> April 2025

Revised: 30<sup>th</sup> May 2025

Accepted: 16<sup>th</sup> June 2025

Published: 30<sup>th</sup> June 2025

### Keywords

Nanostructured lipid carriers (NLCs), Ocular drug delivery, Moxifloxacin, Dexamethasone, Release Kinetics

### ABSTRACT

**Background:** The combination of moxifloxacin hydrochloride (MOX) and dexamethasone sodium phosphate (DEX) is widely available in the conventional commercial market for treating ocular infections and inflammations. Traditional ocular delivery systems are inferior to nanostructured lipid carriers (NLCs) due to their poor drug bioavailability, rapid tear drainage, and limited drug penetration. In contrast, NLCs offer sustained release, enhanced corneal absorption, and improved drug stability. Thus, the research aims to develop moxifloxacin and dexamethasone-loaded NLC for effective drug release. **Methodology:** In this study, a combination of MOX and DEX drugs was loaded in an NLC. The NLC was prepared using standard methods and evaluated for characteristic properties, including particle size (PS), polydispersity index (PDI), entrapment efficiency (EE), and drug loading (DL), as well as drug encapsulation and in vitro studies. **Results and Discussion:** The optimized formulation of NLC possessed a particle size of 190.58 nm and a polydispersity index of 26.7%. The fabricated drug exhibited a KP model release kinetics, indicating that drug release occurred via a combination of diffusion and polymer reaction. The NLC also exhibited a PDI of 26.7%, suggesting a moderately uniform particle size distribution, which further indicates consistent particle size, an acceptable characteristic for nano-carrier systems. The FT-IR analysis revealed optimal encapsulation of drugs inside the lipids, thereby achieving the desired objectives of drug fabrication. **Conclusion:** The formulated NLC has a particle size that falls within the ideal range for a smooth surface in commercial NLC formulations. Additionally, the prepared NLCs' adherence to the KP model underscores their potential as an advanced drug delivery system.

### INTRODUCTION

Bacterial ocular infections are a significant public health concern in India, given the country's diverse climatic conditions, dense population, and variations in hygiene practices [1]. Indian environmental conditions, which are a perfect cocktail mix of

elevated humidity, ambient temperatures above room temperature, and a constant moderate to severe air quality index (AQI), offer ideal breeding conditions for microorganisms [2]. Bacteria such as *Haemophilus influenzae*, *Streptococcus pneumoniae*, *Moraxella catarrhalis*, *Staphylococcus aureus*,

\*University Institute of Pharmacy, Pt. Ravishankar Shukla University, Raipur (C.G.), India

\*For Correspondence: [suresh.preeti@gmail.com](mailto:suresh.preeti@gmail.com)

©2025 The authors

This is an Open Access article distributed under the terms of the Creative Commons Attribution (CC BY NC), which permits unrestricted use, distribution, and reproduction in any medium, as long as the original authors and source are cited. No permission is required from the authors or the publishers. (<https://creativecommons.org/licenses/by-nc/4.0/>)

*Streptococci*, *Escherichia coli*, and *Bacillus cereus* multiply easily in these favourable conditions within a suitable host, leading to infections of vivid severities [3]. These infections can range from mild conjunctivitis to severe conditions, such as keratitis and endophthalmitis, which can lead to vision loss if left untreated. Bacterial conjunctivitis, which is a prevalent ocular condition in India, is often caused by *Staphylococcus aureus*, *Streptococcus pneumoniae*, and *Haemophilus influenzae* [4]. This is characterized by redness, discharge, and irritation. Another prevalent condition is keratitis, where bacteria like *Pseudomonas aeruginosa* and *Staphylococcus aureus* are known to invade the corneal tissue [5]. The country also sees a higher incidence of trachoma, a chronic conjunctival infection caused by *Chlamydia trachomatis*, particularly in rural areas [6]. Additionally, endophthalmitis, a severe intraocular infection caused by bacteria such as Coagulase-negative Staphylococci or Enterococcus species, often occurs post-surgery, especially after cataract surgery, which is widely performed in the country [7]. Poor surgical asepsis and delayed treatment can escalate this condition, leading to irreversible blindness. The prevalence of these infections is heightened by factors such as high temperatures, increased exposure to dust, and agricultural occupations that increase the risk of eye trauma. The widespread use of antibiotics has also led to the emergence of resistance, complicating treatment protocols.

Moxifloxacin and dexamethasone are commonly used together in ocular treatments to address infections and inflammation in the eyes [8]. Moxifloxacin, a 4<sup>th</sup> generation fluoroquinolone antibiotic, is effective in treating bacterial eye infections, such as conjunctivitis, keratitis, and blepharitis [9]. The antibiotic works by inhibiting bacterial DNA gyrase and topoisomerase IV, essential enzymes for bacterial DNA replication, repair, and transcription. It is known for its broad-spectrum activity against both Gram-positive and Gram-negative bacteria. Thus, it becomes helpful in combating common pathogens, such as *Staphylococcus aureus* and *Pseudomonas aeruginosa*. Moxifloxacin is also often prescribed prophylactically before and after ocular surgeries, such as cataract surgery, to prevent post-operative infections.

Dexamethasone, on the other hand, is a potent corticosteroid used to manage ocular inflammation [10]. It works by suppressing the immune response, reducing swelling, redness, and discomfort in inflammatory conditions such as uveitis,

scleritis, or post-surgical inflammation [11]. When combined with moxifloxacin in a single formulation, dexamethasone is known to enhance the effects of the antibiotic used. This combination is widely used in eye drops for conditions that require both antimicrobial and anti-inflammatory effects, such as bacterial keratitis or post-surgical prophylaxis. Medical practitioners always recommend careful monitoring of this drug when used. Its prolonged application can suppress the immune defence system and potentially worsen or mask underlying infections.

The combination of moxifloxacin and dexamethasone is chosen in the study due to its advantage for the preparation of nanostructured lipid carrier (NLC)-based ocular drug delivery systems [12]. Moxifloxacin Hydrochloride is a hydrophilic, broad-spectrum fluoroquinolone with good aqueous solubility, while Dexamethasone Sodium Phosphate is a water-soluble corticosteroid prodrug with anti-inflammatory properties. Their differing but complementary physicochemical profiles—Moxifloxacin's moderate lipophilicity and Dexamethasone's amphiphilic nature—make them well-suited for combined NLC preparation, where the lipid matrix can effectively encapsulate both drugs, enhancing ocular bioavailability and sustained release. Together, these two drugs address both the microbial and inflammatory components of ocular conditions, providing thorough treatment. Incorporating these drugs into an NLC system enhances their delivery to ocular tissues by overcoming the anatomical and physiological barriers of the eye, such as the corneal epithelium and tear clearance. NLCs, with their solid lipid core and liquid lipid shell, offer high drug-loading capacity, sustained release, and improved bioavailability. These properties ensure that therapeutic levels of moxifloxacin and dexamethasone are maintained at the site of action for extended periods, reducing dosing frequency and enhancing patient compliance [13]. Additionally, the lipophilic nature of NLCs facilitates better penetration of these drugs through the lipid-rich barriers of the eye, while protecting them from degradation in the aqueous tear film [14]. This combination, delivered through an NLC system, represents an innovative and efficient approach for managing bacterial ocular infections with associated inflammation, ensuring rapid and sustained therapeutic effects [15]. This study aimed to develop a moxifloxacin and dexamethasone (a combination widely used for treating conjunctivitis) loaded NLC (Dexamethasone MOX-NLC) to enhance permeation through the cornea, while also increasing

the washout period. Thereby, increasing the chances of better eye compatibility. The research work focuses on the preparation of dual-drug-loaded NLCs, whereas existing works primarily focus on single-drug-loaded NLCs. Thus, an attempt has been made to develop a formula that offers optimized NLC properties, with simultaneous antibacterial and anti-inflammatory effects.

### MATERIALS AND METHODS

Akums Drugs and Pharmaceutical Limited, Haridwar, Uttarakhand, India, provided the samples for Moxifloxacin Hydrochloride (hereafter referred to as MOX) and Dexamethasone Sodium Phosphate (hereafter referred to as DEX). The samples were provided free of charge for academic purposes. Stearic acid was procured from Finar Chemicals, Ahmedabad, Gujarat (India), while Oleic acid and Tween 80 were sourced from Merck Life Science Private Limited, Mumbai. Additionally, all other chemicals, including Sodium chloride, Sodium bicarbonate, Sodium hydroxide, and Calcium chloride, were of analytical grade and were supplied by Kasliwal Brothers, Raipur.

### Analytical Method Validation

The UV spectrophotometric method developed was validated by the International Conference on Harmonization (ICH)

guidelines [16]. The calibration curve for both drugs showed a strong linear relationship across the range of 2 to 32 µg/mL. Specificity analysis revealed placebo interference at 1.3% for MOX and 1.4% for DEX, both of which remained below the permissible 2% threshold. Precision was confirmed by low interday and intraday coefficients of variation, all of which were within 2%. Recovery experiments were conducted at 70%, 100%, and 130% concentration levels, each performed three times, with mean recovery values displaying a relative standard deviation (RSD) of less than 2%.

### NLC Experimentation Design

In this study, the Box-Behnken statistical design was utilized [17]. It involved three factors, three levels, and 17 experimental runs for optimization, using Minitab. The independent variables in this research work were surfactant concentration (%w/v) designated as (A), total lipid concentration (%w/v) designated as (B), and the ratio of liquid lipid to total lipid designated as (C) [18]. These variables were assigned high, medium, and low levels based on the outcomes of preliminary experiments. Table 1 provides the coded values for each variable. Following the design, 17 NLC formulations were prepared and evaluated for particle size (R1) and polydispersity index (PDI) (R2), which were designated as response parameters (Table 1).

**Table 1: Adopted Box – Behnken Design for the study along with the Predictor and Predicted Variables**

Variables	Variable Name	Desired Characteristics	
		Base Characteristics	Ceiling Characteristics
Predictor/Independent variables	A = Surfactant concentration (%w/v)	4%	6%
	B = Total lipid concentration (%w/v)	2%	6%
	C = liquid lipid/total lipid	0.2	0.8
Dependent Variables	PS = Particle Size (nm)	Should be less	
	PDI = Polydispersity Index	Should be as close as possible to zero	

### Selection of Liquid Lipid (Oils)

The solubility of Moxifloxacin (MOX) and Dexamethasone (DEX) in various oils was checked. Multiple oils were included, such as Capmul MCM, oleic acid, castor oil, almond oil, and sesame oil. The solubility check was conducted by adding an excess of the drugs to 1 mL of each oil in sealed vials. These vials were placed on a mechanical shaker and maintained at 25 ± 0.2 °C for 72 hrs to reach equilibrium. Following this, the mixtures were centrifuged at 500 rpm for 30 minutes at the same temperature using a high-speed centrifuge, Eppendorf 5430 R. The supernatant was separated and dissolved in methanol, and the solubility was analysed using a Shimadzu UV-1800

spectrophotometer at wavelengths of 287 nm and 242 nm. Each solubility study was conducted in triplicate, and the standard deviation of the data was reported.

### Selection of Solid Lipid

To determine the solubility of MOX and DEX in solid lipids, such as stearic acid (melting point 69 ± 2°C) and Precirol ATO 5 (melting point 60 ± 2°C), 1 mg of each drug was incrementally added to 1 g of melted solid lipid (heated 5°C above its melting point) until it failed to dissolve [19]. The quantity of drugs completely dissolved in the solid lipid was recorded. This experiment was conducted in triplicate for accuracy.

### Selection of a Binary Mixture of Lipids

Solid (Stearic acid) and liquid (Oleic acid) lipids were blended in ratios of -1, 0, and 1 to evaluate their miscibility visually. The liquid mixtures were stirred at 200 rpm for 1 hour at  $75 \pm 0.2^\circ\text{C}$  using a magnetic stirrer (Remi Instruments Ltd., Mumbai, India). The samples were then stored at room temperature for 24 hours before further analysis. A binary mixture exhibiting a melting point above  $75 \pm 0.2^\circ\text{C}$  was selected for its solid-state characteristics.

### Surfactant Selection for Primary Emulsion

The primary emulsion was prepared by combining the selected lipids that exhibited the best miscibility, along with various surfactants, to create a stable formulation [20]. This process involved carefully melting the lipid mixture at  $62^\circ\text{C}$ , followed by the gradual addition of the preheated and agitated surfactant solution. The surfactant solution was slowly incorporated into the lipid mixture using a magnetic stirrer, ensuring thorough blending. The combined solution was continuously stirred for 30 minutes to promote uniform mixing. Afterward, the mixture was allowed to rest for 3 days, during which its stability and clarity were observed and assessed [21]. This procedure was repeated in triplicate to ensure consistency and accuracy of the results. The formulation's stability over time was carefully monitored to ensure it maintained its desired characteristics without phase separation or significant changes in clarity.

### NLC Fabrication

The NLC was prepared using a modified version of the melt-emulsification. In brief, a mixture of solid and liquid lipids was heated to a temperature of  $62^\circ\text{C} \pm 2^\circ\text{C}$ , which is  $5^\circ\text{C}$  above the melting point of the solid lipid. During this phase, the drugs MOX and DEX were incorporated into the melted lipid mixture. An aqueous surfactant solution, preheated to  $85^\circ\text{C}$ , was then added dropwise to the lipid mixture with the aid of a mechanical stirrer, forming the primary emulsion. This primary emulsion was further processed using an ultrasonic probe sonicator (Altrasonics, Mumbai, India) for 15 minutes to achieve a homogeneous nanoemulsion. Afterward, the nanoemulsion was rapidly cooled in an ice bath to solidify the lipid matrix and produce the NLC [22], as schematically presented in Figure 1.

### Particle Size and Polydispersity Index

The average particle size and polydispersity index (PDI) of the NLC formulation were measured using dynamic light scattering

(DLS) with a Zetasizer model Litesizer DLS 500 (Anton Paar, USA) at a temperature of  $25 \pm 0.2^\circ\text{C}$ . Prior to analysis, the formulation was diluted 100 times to achieve an optimal scattering intensity. A consistent sample volume of 1 ml was used for the measurements. This instrument was used explicitly because it was equipped with specialized software that was designed for the analysis of particle size and PDI measurement.

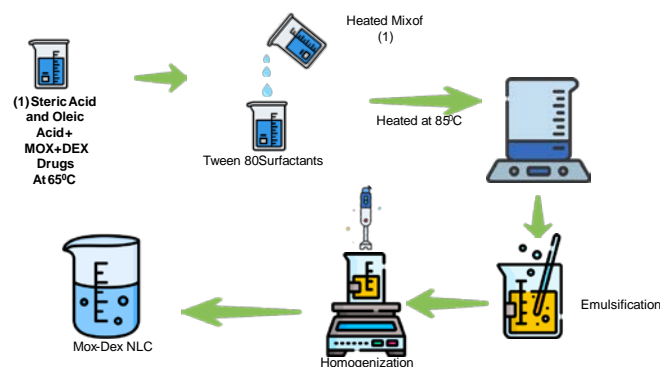


**Figure 1: Schematic presentation of NLC preparation**

### Transmission Electron Microscopy (TEM)

The surface morphology of the prepared NLC was examined using Transmission Electron Microscopy (TEM) (Morgagni 268D TEM, Massachusetts, USA) to observe the detailed structure at the nanoscale. A small drop of the NLC dispersion was carefully placed on a paraffin sheet, and a carbon-coated grid was gently positioned on top of the sample. The sample was left for 1 minute to ensure that the NLC particles adhered firmly to the carbon surface. To remove any excess drug, the remaining sample was carefully blotted using a piece of filter paper. Following this, the grid was immersed in a 1% phosphotungstate solution for 10 seconds to stain the NLC particles, enhancing the contrast for better visualization [23]. After this staining step, the excess liquid was removed by blotting with filter paper, and the sample was left to air dry. Once dried, the prepared sample was analyzed under the TEM to study the surface morphology and confirm the nanoscale characteristics of the NLC formulation. This detailed process ensured accurate imaging for further analysis of the NLC structure.

### FT-IR

A quantity of KBr (0.3 g), which had been previously dried at  $250^\circ\text{C}$  for 1 hour and allowed to cool to room temperature, was carefully weighed and then powdered. Then, 2 mg of each test sample, including MOX, DEX, Stearic acid, and the optimized

NLC formulation, were added to the powdered KBr [24]. The components were thoroughly mixed to achieve a homogeneous blend, which was then finely ground to ensure uniformity. A small portion of this powder mixture was taken and compressed under pressure to form a thin, semi-transparent pellet. The resulting pellet was subjected to infrared (IR) spectroscopy to record its spectrum and analyze the molecular vibrations of the samples. This method enabled the detailed examination of the functional groups present in the samples. The IR spectrum was recorded using the appropriate equipment, allowing for further structural analysis and comparison of the individual components and their interactions within the NLC formulation.

### Entrapment Efficiency and Drug Loading

To evaluate the entrapment efficiency of drug-loaded NLCs, the formulations were centrifuged at 30,000 rpm for 1 hour in an ultracentrifuge. After centrifugation, the supernatant was diluted with methanol and analyzed spectrophotometrically at 287 nm and 242 nm, respectively. The following equation was used to calculate the entrapment efficiency (in % by weight).

$$\text{Entrapment Efficiency (\%)} = \frac{\text{Total Drug} - \text{Free Drug}}{\text{Total Drug}} \times 100$$

$$\text{Drug Loading} = \frac{\text{Total Drug} - \text{Free Drug}}{\text{Weight of lipids}} \times 100$$

Where, Total drug = amount of drug present in prepared formulation in mg, Free Drug = amount of drug unentrapped in prepared NLC in mg

### In vitro Testing

Dialysis membrane technology was employed to evaluate the in vitro release profile of drugs from the NLC formulations [27]. Before use, the dialysis membrane underwent an activation process to ensure it was ready for the experiment. Subsequently, 1 ml of the NLC formulation and drug suspension were separately transferred into pre-activated dialysis bags (molecular weight cutoff of 12,000 g/mol, procured from Sigma Aldrich Chemicals, Pvt. Ltd., Missouri, USA). These bags were carefully suspended in 100 ml of phosphate buffer saline (PBS) with a pH of 7.4, maintained at a constant temperature of  $37 \pm 2^\circ\text{C}$  to simulate physiological conditions. The system was kept under continuous stirring using a magnetic stirrer set at 150 rpm, with separate assemblies for each formulation. At specific time intervals, aliquots were meticulously withdrawn from the release medium, and the same volume of fresh phosphate buffer was added to maintain sink conditions and ensure consistent drug

diffusion. The withdrawn aliquots were analyzed to quantify the drug release, with MOX and DEX measured spectrophotometrically at wavelengths of 287 nm and 242 nm, respectively. This method ensured precise and accurate measurement of drug release over time [28]. Each experiment was conducted in triplicate to ensure the reproducibility and reliability of the results. This rigorous protocol enabled a comprehensive understanding of the release behavior of drugs from NLC formulations.

### Drug release

The data obtained from the in vitro release studies of MOX and DEX-loaded NLCs were analyzed using various kinetic models to understand the drug release mechanism [29]. These models included zero-order (fraction of drug released versus time), first-order (log percentage of drug remaining versus time), the Higuchi model (fraction of drug released versus the square root of time), the Korsmeyer-Peppas model ( $r=Kt^n$  where r represents the percentage of drug released, K is the kinetic constant, and n is the release exponent that indicates the release mechanism), and the Hixson-Crowell model (cube root of the percentage of drug remaining versus time) [30]. The coefficient of correlation ( $R^2$ ) values were calculated based on the linear curves derived through regression analysis of the respective plots. Additionally, the value of n was determined from the slope of the Korsmeyer-Peppas model. An nnn-value of 0.43 or lower suggests that the drug release follows a Fickian diffusion mechanism, while an nnn-value between 0.43 and 0.85 indicates a non-Fickian release mechanism [31]. When nnn equals 0.85, the drug release is consistent with a zero-order mechanism. This analysis helps to elucidate the pattern and behavior of drug release from the NLC formulations.

## RESULTS AND DISCUSSION

### Selection of excipients

To develop MOX and DEX-loaded NLCs, the excipients need to meet specific criteria, such as being pharmacologically acceptable, non-irritating, and free from ocular sensitization properties. The excipients chosen for solubility studies were classified as Generally Recognized as Safe (GRAS). Results from the solubility experiments revealed that stearic acid provided the highest solubility for MOX and DEX among the solid lipids, measuring  $6 \pm 0.61$  mg/mL and  $5 \pm 0.53$  mg/mL, respectively. Similarly, oleic acid showed the most excellent solubility among liquid lipids, with values of  $5 \pm 0.04$  mg/ml and

$6 \pm 0.60$  mg/ml for MOX and DEX, respectively. Based on these findings, stearic acid and oleic acid were selected as the solid and liquid lipids, respectively. Different ratios of solid to liquid lipids, such as 1:1, 1:2, and 2:1, were tested, and the optimal observation was achieved with a 1:2 ratio. Consequently, a 1:2 ratio of stearic acid and oleic acid was used as the binary lipid phase for NLC formulation development.

The surfactant was chosen based on the stability and clarity of the primary emulsion formed during the experiments. Tween 80, within a concentration range of 4–6% (w/v), was determined to be the most suitable for fabricating the NLC formulation. This combination of lipids and surfactant ensured the stability and efficacy of the final NLC product.

### FABRICATION & OPTIMIZATION OF NLC

Based on the specified constraints for each independent variable (A, B, and C, as mentioned in Table 1), the Minitab software generated an optimized formulation autonomously. The details of the generated optimized formulation have been presented in Table 2. Seventeen batches of drug-loaded NLCs were prepared to validate this optimization, with experimental values obtained by evaluating the response parameters, such as particle size and PDI, as per the software-generated formula. In the table formulations, NH13 to NH17 are identical because of the adopted Box-Behnken design. This replication aids in estimating experimental error, enhances the robustness of the model, establishes the reproducibility of the formulation, and improves predictive power. The percentage prediction was calculated to assess the software's accuracy and the effectiveness of the experimental design in tailoring the NLCs to achieve the desired characteristics.

When the experimental response values from the 17 runs were analyzed across various models, including the Box-Behnken design, the quadratic model was identified as the best fit for all three dependent variables, with a coefficient of determination ( $R^2$ ) nearly equal to 1, indicating excellent predictive capability. The significance of F for both equations was observed as less than 0.01. This suggests that the model is valid for predicting particle size and PDI. The p-value associated with A, B, C, AB, BC, CA,  $A^2$ ,  $B^2$ , and  $C^2$  was less than 0.01, indicating a significant relationship between the variables of interest. The determined models through polynomial curve fitting are as presented below:

$$PS = -66.35 + 33.89A + 86.79B - 77.93C + 5.18A^2 + 8.82B^2 + 88.39C^2 - 17.15AB - 0.35AC - 4.54BC \quad (R^2 = 0.997)$$

$$PDI = -2.43 + 3.84A + 9.91B - 9.69C + 0.68A^2 + 1.13B^2 + 11.11C^2 - 2.16AB - 0.04AC - 0.63BC \quad (R^2 = 0.996)$$

Figure 2 shows the response surface 3D plot showing the effect of surfactant concentration and lipid ratio on particle size, while Figure 3 shows the response surface 3D plot showing the effect of surfactant concentration and liquid lipid concentration on polydispersity index. Using the fitting equations 1 and 2, values of PS and PDI were predicted. The observed vs predicted values are plotted in Figure 4. From the deduced results, it is evident that lower lipid and surfactant concentrations lead to smaller particle sizes. This might be because there is less material to form larger particles. Thus, less material coalesces into bigger droplets [32].

The predicted particle size obtained through the equation was closer to the actual particle size, as shown in Figure 4(a). Similarly, the predicted PDI, as calculated using Equation 2, was closer to the actual PDI, as shown in Figure 4(b). This suggests that design parameters could be chosen for the formulation of NLC. Based on this, the parameters A, B, and C were selected for NLC formulation, where the PDI values are closer to zero and the particle size is smaller as compared to the others. This was performed to maintain moderately polydispersity, which is essential for ocular medicine formulation. Thus, the NH2 formulation was selected for the preparation of NLCs.

### Particle size

The determination of particle size and polydispersity index was repeated for all 17 samples, as listed in Table 2. However, a discussion has been presented only for sample NH2 as it possessed the smallest particle size and lowest polydispersity index. Based on equations 1 and 2, it can be said that parameters A, B, and C play an important role in altering the particle size and polydispersity index. The particle size and polydispersity index for the selected formulation (NH2) were obtained as 190.58 nm and 26.7% respectively. This is shown in Figure 5. Earlier studies have indicated that the NLC particle size should be within the range of 10 to 1000 nm to prevent it from being considered a foreign body by ocular tissues [22,33]. Furthermore, this particle size also allows for the effective passage of drugs that are poorly water-soluble through ocular tissues [34].

**Table 2: Box Behnken-based experimental design for optimised formulation of NLC**

Code for prepared Formulation	Surfactant Concentration% (A)	Lipid Concentration% (B)	Lipid Ratio (C)	Particle Size PS (nm)	Polydispersity Index PDI (%)
NH1	4	6	0.5	543.13	67.41
NH2	4	2	0.5	190.58	26.7
NH3	6	2	0.5	308.67	41.07
NH4	6	6	0.5	524.06	64.47
NH5	4	4	0.2	356.99	45.63
NH6	4	4	0.8	353.35	45.12
NH7	6	4	0.2	375.45	47.7
NH8	6	4	0.8	371.39	47.14
NH9	5	2	0.2	260.04	35.17
NH10	5	2	0.8	257.99	34.88
NH11	5	6	0.2	536.23	66.35
NH12	5	6	0.8	523.28	64.54
NH13	5	4	0.5	351.16	44.72
NH14	5	4	0.5	351.16	44.72
NH15	5	4	0.5	351.16	44.72
NH16	5	4	0.5	351.16	44.72
NH17	5	4	0.5	351.16	44.72

Response Surface: PS vs A & C

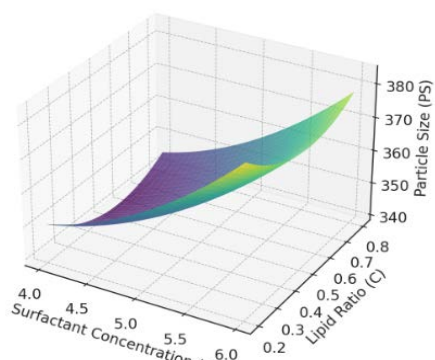


**Figure 2: Response surface 3D plot showing the effect of surfactant concentration and lipid ratio on particle size**

Response Surface: PDI vs A & B

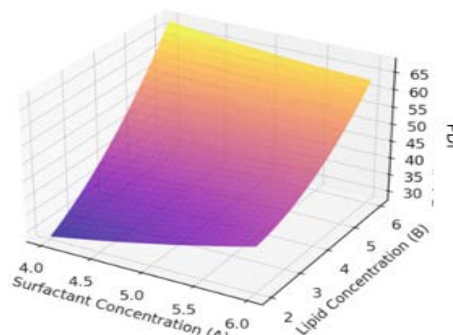


**Figure 3: Response surface 3D plot showing the effect of surfactant concentration & lipid ratio on polydispersity index**

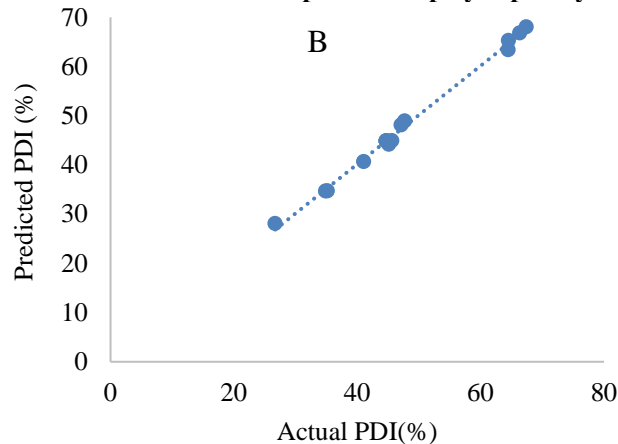
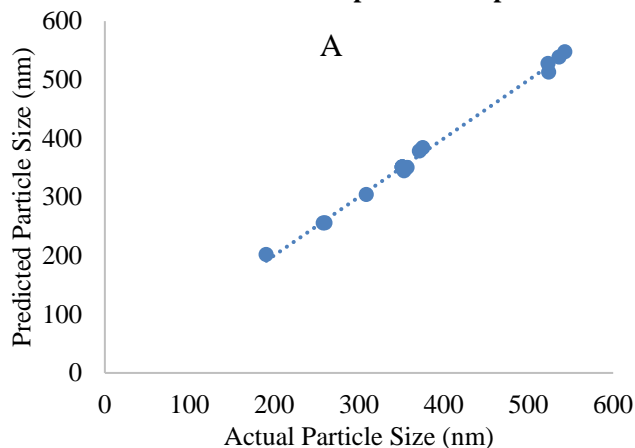


**Figure 4: Linear relationship fit between the two variables for establishment of good design parameters (a) Predicted Vs. Actual Particle Size, (b) Predicted Vs. Actual Polydispersity Index**

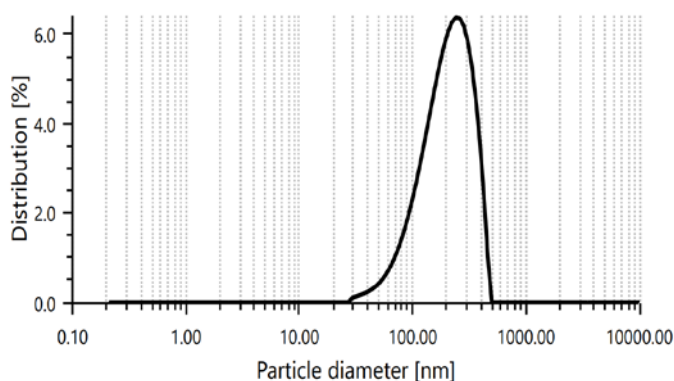


**Figure 5: Particle size distribution of selected optimized NLC (NH2) formulation**

The TEM image of NLC, as shown in Figure 6, revealed a spherical and smooth-surfaced lipid nanoparticle. The particle determined by TEM photomicrograph was 178.21 nm. This was consistent with the particle size of 190.58 nm determined by the Zetasizer. The next step in the fabrication formulation was to perform FTIR spectral analysis. FTIR spectral analysis was performed to ensure that complete encapsulation of MOX-DEX

had been achieved inside the NLC. Figure 7a shows the FT-IR spectrum for MOX, 7b shows the FT-IR for DEX, 7c shows the FT-IR for stearic acid, and 7d shows the FT-IR for NLC.

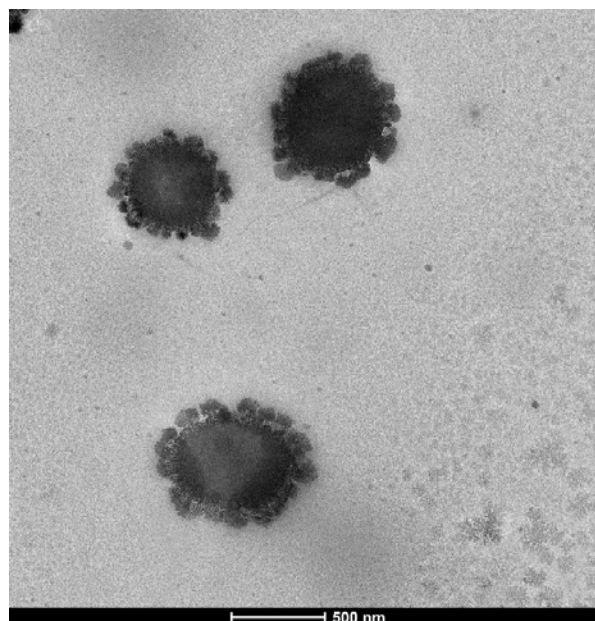
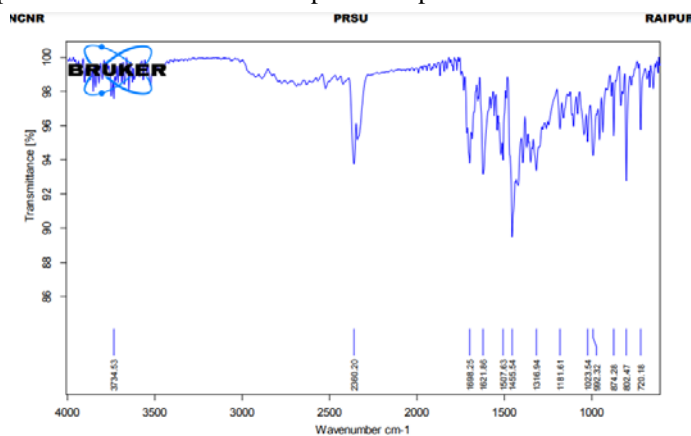
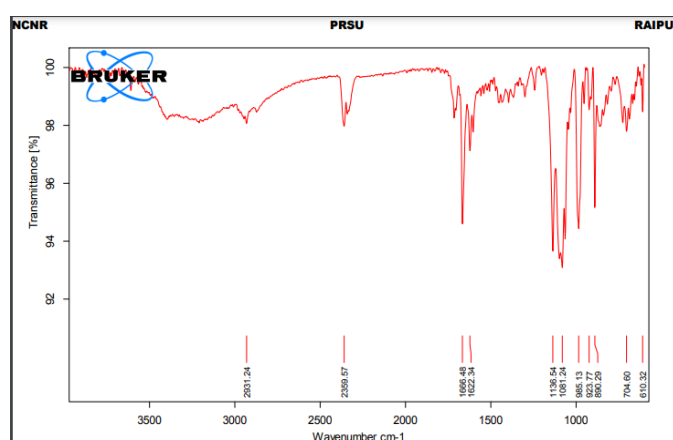


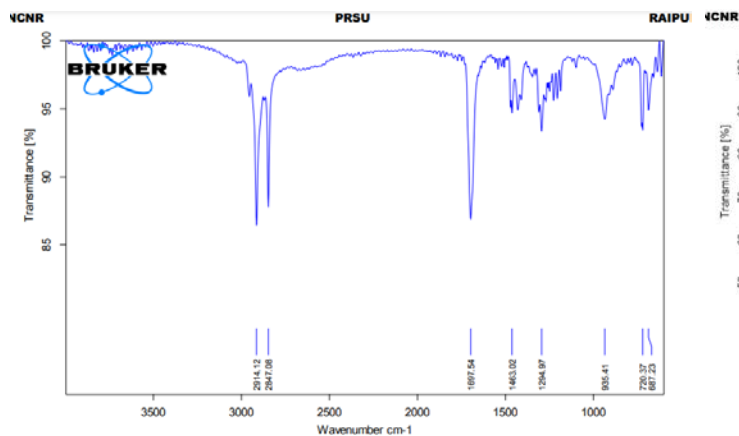
**Figure 6: TEM Image of optimized NLC**



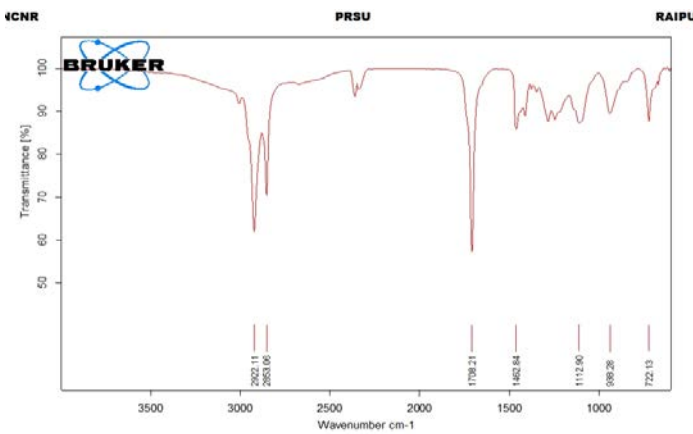
(a)



(b)



(c)



(d)

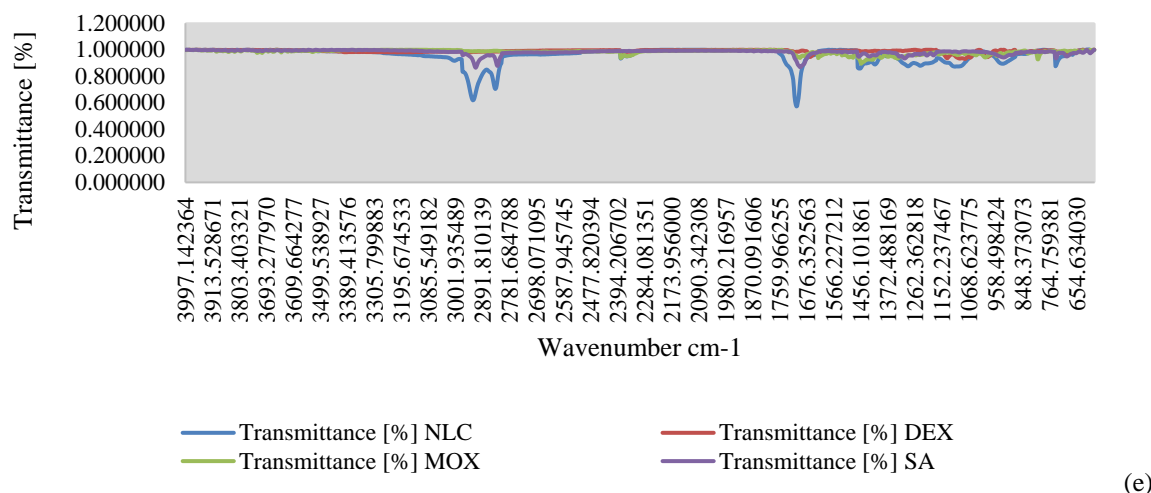


**Figure 7: The FT-IR of (a) MOX, (b) DEX, (c) stearic acid, (d) NLC, (e) combined visualization**

From Figure 7, it is evident that the FT-IR peaks for MOX are observed at wavenumbers 3734.53, 2360.20, and 1698.25. For DEX, peaks were observed at wavenumbers 2931.24, 2359.57, and 1666.48. For stearic acid, the peaks were observed at wavenumbers 2914.12, 2847.08, and 1697.54. The FT-IR spectrum of NLC exhibits peaks at wavenumbers 2922.11, 2853.06, and 1708.21, which are distinctly different from those observed for MOX and DEX. This confirms complete encapsulation of drugs under NLC for effective delivery [35]. The entrapment efficiency (EE) of the optimized NLC formulation (NH2) for MOX and DEX was determined to be  $80.09 \pm 0.32\%$  and  $72.38 \pm 0.31\%$ , respectively, while the drug loading (DL) for the same formulation was  $5.6 \pm 0.012\%$  for MOX and  $7.66 \pm 0.01\%$  for DEX. Achieving simultaneous encapsulation of both MOX and DEX within the NLC matrix presented a significant challenge. This encapsulation depended primarily on the concentration of the drugs, the optimized ratio of solid & liquid lipids & the concentration of the surfactant used [36]. The results for EE and DL of both drugs were comparable.

Despite the hydrophilic nature of MOX, its low dosage allowed for effective encapsulation in the NLC. Studies have shown that high entrapment efficiency can be achieved by incorporating hydrophilic drugs within the surfactant layer on the surface of lipid carriers. In contrast, corticosteroid-type drugs are encapsulated within the lipid core of the NLC [20,37]. During the formation of the microemulsion, drugs may migrate from the oil phase to the aqueous phase. However, as the microemulsion cools, the solubility of the drugs in the aqueous phase decreases, causing them to re-partition into the lipid phase. As the

temperature decreases further, the solid lipid core begins to form, encapsulating the drugs from the liquid phase. This process concentrates the drug molecules either in the outer liquid layer of the NLC or on the particle surface, contributing to effective encapsulation and loading [38].

### Release Kinetics

To study the drug release kinetics of the prepared NLC, an *in vitro* study was conducted. Through experimental results, various drug release kinetic models were fitted to the obtained data. The primary objective of fitting various kinetic models to the received data was to determine the optimal  $R^2$  value or the best correlation coefficient between time and the drug release parameter. To better understand the drug release kinetics of the prepared NLC, it was subjected to different kinetic models. The determined  $R^2$  values of various models for the NLC are presented in Table 3.

**Table 3:  $R^2$  value determined for different kinetic models for prepared NLC**

Model	Determined $R^2$
Zero Order	0.9939
First Order	0.9975
Higuchi Model	0.9922
Korsmeyer Peppas Model	0.9989

Table 3 indicates that the highest  $R^2$  value is obtained for the Korsmeyer-Peppas (KP) model release. The high  $R^2$  value obtained for the Korsmeyer-Peppas (KP) model suggests that this model best describes the drug release kinetics of the

Moxifloxacin-Dexamethasone-loaded NLC system. The KP model is particularly suitable for systems where a combination of diffusion and polymer relaxation regulates drug release. The  $n$ -value in the KP model also provides insights into the release mechanism, such as Fickian diffusion ( $n < 0.5$ ) or anomalous transport ( $0.5 < n < 1$ ). For the formulated NLC, the  $n$  value was determined to be 0.86, indicating high possibilities of non-Fickian transport [39]. This suggests that the release mechanism for the NLC is likely a complex interplay of diffusion and erosion, rather than being solely dependent on either factor [40].

The order of  $R^2$  values—KP model, first-order, zero-order, and Higuchi—highlights the complexity of the drug release system. The relatively high  $R^2$  of the first-order model indicates that drug release is concentration-dependent. In contrast, the zero-order model suggests that sustained and consistent release is less significant in this system. The Higuchi model's lower  $R^2$  implies that diffusion alone cannot fully account for the release behavior. Overall, the results affirm that the KP model provides a comprehensive description of the NLC's drug release dynamics, reflecting the influence of both drug diffusion and the structural properties of the lipid carrier matrix.

### CONCLUSION

The Nanostructured Lipid Carrier (NLC) formulation of moxifloxacin and dexamethasone prepared with stearic acid and oleic acid successfully demonstrated its potential for anomalous drug release. The average particle size observed by Transmission Electron Microscopy (TEM) was 178.21 nm. In comparison, the Zetasizer analysis revealed a slightly larger size of 190.58 nm with a polydispersity index (PDI) of 26.7%, indicating a relatively broad size distribution. The NLC formulation showed KP model release kinetics, suggesting that the drug is a complex phenomenon.

The particle sizes observed by TEM and Zetasizer were comparable, with a slight discrepancy between the two methods, which is often due to differences in the techniques. TEM provides a visual representation of individual particles. In contrast, the Zetasizer measures the hydrodynamic diameter in a dispersed environment, which accounts for hydration layers and may result in a larger size measurement. The polydispersity index (PDI) of 26.7% indicates a moderate degree of size distribution, which is not ideal but is typical for specific lipid-based formulations. A more uniform particle size distribution

could improve the reproducibility of drug release. Nevertheless, the particle size range observed (approximately 190 nm) falls within the typical range for NLC formulations, supporting its potential use in drug delivery systems targeting systemic or localized therapies.

The study demonstrates that the particle size and polydispersity index (PDI) of Moxifloxacin-Dexamethasone-loaded nanostructured lipid carriers (NLCs) are significantly influenced by the surfactant-to-lipid ratios. The smallest particle size and most favorable PDI were achieved at lower surfactant and lipid ratios, suggesting that reduced surfactant concentration minimizes particle aggregation. In contrast, a balanced lipid ratio promotes efficient emulsification. In contrast, higher surfactant and lipid ratios resulted in larger particle sizes, potentially due to the formation of coarser emulsions or excess surfactant interfering with particle stabilization. Furthermore, the drug release kinetics of the prepared NLCs followed the Korsmeyer-Peppas (KP) model, indicating that the release mechanism involves a combination of diffusion and matrix erosion, which reflects the complex interplay between the lipid matrix and drug diffusion behavior.

The NLC's adherence to the KP model underscores its potential as an advanced drug delivery system. The model's applicability is particularly relevant for NLCs due to their unique structure, which ensures sustained release through the solid lipid matrix. In contrast, the liquid lipid fraction promotes drug solubilization and mobility [41]. By providing insight into the diffusion-based and structural release mechanisms, the KP model offers a predictive framework for optimizing NLC formulations to achieve efficient drug delivery. Patient compliance is a crucial factor in ocular treatments.

This anomalous release behavior is particularly advantageous for ocular or systemic drug delivery, as it allows for sustained therapeutic effects, i.e., the drug being released over a period through a combination of diffusion and matrix erosion, thereby reducing the dosing frequency and improving patient compliance [42]. The formulation prepared exhibits promise for effective ocular drug delivery; however, the study was limited to the development of the formulation only, and the analysis of ocular toxicity, irritation in biological models, and feasibility of scaling this to commercial production levels remains to be tested. Overall, these findings underscore the crucial role of

formulation parameters in tailoring the physicochemical properties and release kinetics of NLCs, thereby facilitating their effective application in pharmaceutical development.

#### FINANCIAL ASSISTANCE

NIL

#### CONFLICT OF INTEREST

The authors declare no conflict of interest.

#### AUTHOR CONTRIBUTION

Narayan Hemnani conceptualized the study, performed the formulation and characterization experiments, and contributed to data analysis and manuscript drafting. Preeti K Suresh supervised the research, guided the release kinetics modeling, and critically revised the manuscript for intellectual content. Both authors read and approved the final manuscript.

#### REFERENCES

- [1] Bharathi Mj, Amuthan M, Viswanathan S, Ramesh S, Ramakrishnan R. Prevalence of bacterial pathogens causing ocular infections in South India. *Indian J Pathol Microbiol*, **53**, 281 (2010) <https://doi.org/10.4103/0377-4929.64336>.
- [2] Kurmi OP, Adhikari TB, Tyagi SK, Kallestrup P, Sigsgaard T. Addressing air pollution in India: Innovative strategies for sustainable solutions. *Indian J Med Res*, **160**, 1–5 (2024) [https://doi.org/10.25259/IJMR\\_691\\_2024](https://doi.org/10.25259/IJMR_691_2024).
- [3] John TJ, Cherian T, Raghupathy P. Haemophilus influenzae disease in children in India: a hospital perspective: *The Pediatric Infectious Disease Journal*, **17**, S169–71 (1998) <https://doi.org/10.1097/00006454-199809001-00015>.
- [4] Mohanasundaram AS, Gurnani B, Kaur K, Manikkam R. Madras eye outbreak in India: Why should we foster a better understanding of acute conjunctivitis? *Indian Journal of Ophthalmology*, **71**, 2298–9 (2023) [https://doi.org/10.4103/IJO.IJO\\_3317\\_22](https://doi.org/10.4103/IJO.IJO_3317_22).
- [5] Shah S, Wozniak RAF. Staphylococcus aureus and Pseudomonas aeruginosa infectious keratitis: key bacterial mechanisms that mediate pathogenesis and emerging therapeutics. *Front. Cell. Infect. Microbiol.*, **13**, 1250257 (2023) <https://doi.org/10.3389/fcimb.2023.1250257>.
- [6] Satpathy G, Behera H, Ahmed N. Chlamydial eye infections: Current perspectives. *Indian J Ophthalmol*, **65**, 97 (2017) [https://doi.org/10.4103/ijo.IJO\\_870\\_16](https://doi.org/10.4103/ijo.IJO_870_16).
- [7] Michalik M, Samet A, Podbielska-Kubera A, Savini V, Międzobrodzki J, Kosecka-Strojek M. Coagulase-negative staphylococci (CoNS) as a significant etiological factor of laryngological infections: a review. *Ann Clin Microbiol Antimicrob*, **19**, 26 (2020) <https://doi.org/10.1186/s12941-020-00367-x>.
- [8] Drago L. Topical Antibiotic Therapy in the Ocular Environment: The Benefits of Using Moxifloxacin Eyedrops. *Microorganisms*, **12**, 649 (2024) <https://doi.org/10.3390/microorganisms12040649>.
- [9] McCulley JP, Caudle D, Aronowicz JD, Shine WE. Fourth-Generation Fluoroquinolone Penetration into the Aqueous Humor in Humans. *Ophthalmology*, **113**, 955–9 (2006) <https://doi.org/10.1016/j.ophtha.2006.01.061>.
- [10] Lin MX, Guo L, Saldanha IJ, VanCourt S, Zeng J, Karakus S, Hessen M, Li G, Akpek EK. Dexamethasone Intracanalicular Insert for Clinically Significant Aqueous-Deficient Dry Eye. *Ophthalmology*, **131**, 1033–44 (2024) <https://doi.org/10.1016/j.ophtha.2024.03.010>.
- [11] Zheng Q, Ge C, Li K, Wang L, Xia X, Liu X, Mehmood R, Shen J, Nan K, Chen W, Lin S. Remote-controlled dexamethasone-duration on eye-surface with a micelle-magnetic nanoparticulate co-delivery system for dry eye disease. *Acta Pharmaceutica Sinica B*, **14**, 3730–45 (2024) <https://doi.org/10.1016/j.apsb.2024.05.004>.
- [12] L. Kiss E, Berkó S, Gácsi A, Kovács A, Katona G, Soós J, Csányi E, Gróf I, Harazin A, Deli MA, Budai-Szűcs M. Design and Optimization of Nanostructured Lipid Carrier Containing Dexamethasone for Ophthalmic Use. *Pharmaceutics*, **11**, 679 (2019) <https://doi.org/10.3390/pharmaceutics11120679>.
- [13] Lakhani P, Patil A, Taskar P, Ashour E, Majumdar S. Curcumin-loaded Nanostructured Lipid Carriers for ocular drug delivery: Design optimization and characterization. *Journal of Drug Delivery Science and Technology*, **47**, 159–66 (2018) <https://doi.org/10.1016/j.jddst.2018.07.010>.
- [14] Khan S, Sharma A, Jain V. An Overview of Nanostructured Lipid Carriers and its Application in Drug Delivery through Different Routes. *Adv Pharm Bull*, **13**, 446–60 (2023) <https://doi.org/10.34172/apb.2023.056>.
- [15] Baig MS, Karade SK, Ahmad A, Khan MohdA, Haque A, Webster TJ, Faiyazuddin Md, Al-Qahtani NH. Lipid-based nanoparticles: innovations in ocular drug delivery. *Front. Mol. Biosci.*, **11**, 1421959 (2024) <https://doi.org/10.3389/fmolb.2024.1421959>.
- [16] Yan T, Ma Z, Liu J, Yin N, Lei S, Zhang X, Li X, Zhang Y, Kong J. Thermoresponsive GenisteinNLC-dexamethasone-moxifloxacin multi drug delivery system in lens capsule bag to prevent complications after cataract surgery. *Sci Rep*, **11**, 181 (2021) <https://doi.org/10.1038/s41598-020-80476-x>.
- [17] Thapa C, Ahad A, Aqil Mohd, Imam SS, Sultana Y. Formulation and optimization of nanostructured lipid carriers to enhance oral bioavailability of telmisartan using Box–Behnken design. *Journal of Drug Delivery Science and Technology*, **44**, 431–9 (2018) <https://doi.org/10.1016/j.jddst.2018.02.003>.

- [18] Elmowafy M, Al-Sanea MM. Nanostructured lipid carriers (NLCs) as drug delivery platform: Advances in formulation and delivery strategies. *Saudi Pharmaceutical Journal*, **29**, 999–1012 (2021) <https://doi.org/10.1016/j.jsps.2021.07.015>.
- [19] Patel D. Nanostructured Lipid Carriers (NLC)-Based Gel for Topical Delivery of Aceclofenac: Preparation, Characterization and In Vivo Evaluation. *Sci. Pharm.*, **80**, 749–64 (2012) <https://doi.org/10.3797/scipharm.1202-12>.
- [20] Chauhan I, Yasir M, Verma M, Singh AP. Nanostructured Lipid Carriers: A Groundbreaking Approach for Transdermal Drug Delivery. *Adv Pharm Bull*, **10**, 150–65 (2020) <https://doi.org/10.34172/apb.2020.021>.
- [21] Hsueh Y-S, Shyong Y-J, Yu H-C, Jheng S-J, Lin S-W, Wu H-L, Tsai J-C. Nanostructured Lipid Carrier Gel Formulation of Recombinant Human Thrombomodulin Improve Diabetic Wound Healing by Topical Administration. *Pharmaceutics*, **13**, 1386 (2021) <https://doi.org/10.3390/pharmaceutics13091386>.
- [22] Varela-Fernández R, García-Otero X, Díaz-Tomé V, Regueiro U, López-López M, González-Barcia M, Isabel Lema M, Javier Otero-Espinar F. Lactoferrin-loaded nanostructured lipid carriers (NLCs) as a new formulation for optimized ocular drug delivery. *European Journal of Pharmaceutics and Biopharmaceutics*, **172**, 144–56 (2022) <https://doi.org/10.1016/j.ejpb.2022.02.010>.
- [23] Deep A, Kumar M, Pahwa R, Gupta S, Bhatt S, Kumari B, Upadhyay PK, Pandurangan A. Formulation and in vivo pharmacodynamics studies of nanostructured lipid carriers for topical delivery of bifonazole. *actapharm*, **59**, 559 (2021) <https://doi.org/10.23893/1307-2080.APS.05902>.
- [24] Pezeshki A, Ghanbarzadeh B, Mohammadi M, Fathollahi I, Hamishehkar H. Encapsulation of Vitamin A Palmitate in Nanostructured Lipid Carrier (NLC)-Effect of Surfactant Concentration on the Formulation Properties. *Advanced Pharmaceutical Bulletin; eISSN 2251-7308*, (2014) <https://doi.org/10.5681/APB.2014.083>.
- [25] Gilani SJ, Jumah MNB, Zafar A, Imam SS, Yasir M, Khalid M, Alshehri S, Ghuneim MM, Albohairy FM. Formulation and Evaluation of Nano Lipid Carrier-Based Ocular Gel System: Optimization to Antibacterial Activity. *Gels*, **8**, 255 (2022) <https://doi.org/10.3390/gels8050255>.
- [26] Lakhani P, Patil A, Taskar P, Ashour E, Majumdar S. Curcumin-loaded Nanostructured Lipid Carriers for ocular drug delivery: Design optimization and characterization. *Journal of Drug Delivery Science and Technology*, **47**, 159–66 (2018) <https://doi.org/10.1016/j.jddst.2018.07.010>.
- [27] Ortiz AC, Yañez O, Salas-Huenuleo E, Morales JO. Development of a Nanostructured Lipid Carrier (NLC) by a Low-Energy Method, Comparison of Release Kinetics and Molecular Dynamics Simulation. *Pharmaceutics*, **13**, 531 (2021) <https://doi.org/10.3390/pharmaceutics13040531>.
- [28] Gómez-Lázaro L, Martín-Sabroso C, Aparicio-Blanco J, Torres-Suárez AI. Assessment of In Vitro Release Testing Methods for Colloidal Drug Carriers: The Lack of Standardized Protocols. *Pharmaceutics*, **16**, 103 (2024) <https://doi.org/10.3390/pharmaceutics16010103>.
- [29] Ahalwat S, Bhatt DC. Development of novel lipid matrix for improved sustained release effect of a hydrophilic drug via response surface methodology. *Journal of Drug Delivery Science and Technology*, **67**, 102993 (2022) <https://doi.org/10.1016/j.jddst.2021.102993>.
- [30] Pinheiro M, Ribeiro R, Vieira A, Andrade F, Reis S. Design of a nanostructured lipid carrier intended to improve the treatment of tuberculosis. *DDDT*, **Volume 10**, 2467–75 (2016) <https://doi.org/10.2147/DDDT.S104395>.
- [31] Deshkar SS, Jadhav MS, Shirolkar SV. Development of Carbamazepine Nanostructured Lipid Carrier Loaded Thermosensitive Gel for Intranasal Delivery. *Adv Pharm Bull*, **11**, 150–62 (2020) <https://doi.org/10.34172/apb.2021.016>.
- [32] Azhar Shekoufeh Bahari L, Hamishehkar H. The Impact of Variables on Particle Size of Solid Lipid Nanoparticles and Nanostructured Lipid Carriers; A Comparative Literature Review. *Adv Pharm Bull*, **6**, 143–51 (2016) <https://doi.org/10.15171/apb.2016.021>.
- [33] Khosa A, Reddi S, Saha RN. Nanostructured lipid carriers for site-specific drug delivery. *Biomedicine & Pharmacotherapy*, **103**, 598–613 (2018) <https://doi.org/10.1016/j.biopha.2018.04.055>.
- [34] Nguyen VH, Thuy VN, Van TV, Dao AH, Lee B-J. Nanostructured lipid carriers and their potential applications for versatile drug delivery via oral administration. *OpenNano*, **8**, 100064 (2022) <https://doi.org/10.1016/j.onano.2022.100064>.
- [35] Gade S, Patel KK, Gupta C, Anjum MdM, Deepika D, Agrawal AK, Singh S. An Ex Vivo Evaluation of Moxifloxacin Nanostructured Lipid Carrier Enriched In Situ Gel for Transcorneal Permeation on Goat Cornea. *Journal of Pharmaceutical Sciences*, **108**, 2905–16 (2019) <https://doi.org/10.1016/j.xphs.2019.04.005>.
- [36] Joshi PH, Youssef AAA, Ghonge M, Varner C, Tripathi S, Dudhipala N, Majumdar S. Gatifloxacin Loaded Nano Lipid Carriers for the Management of Bacterial Conjunctivitis. *Antibiotics*, **12**, 1318 (2023) <https://doi.org/10.3390/antibiotics12081318>.
- [37] Mall J, Naseem N, Haider MdF, Rahman MA, Khan S, Siddiqui SN. Nanostructured lipid carriers as a drug delivery system: A comprehensive review with therapeutic applications. *Intelligent Pharmacy*, S2949866X24001023 (2024) <https://doi.org/10.1016/j.ipha.2024.09.005>.
- [38] Viegas C, Patrício AB, Prata JM, Nadhman A, Chintamaneni PK, Fonte P. Solid Lipid Nanoparticles vs. Nanostructured Lipid

- Carriers: A Comparative Review. *Pharmaceutics*, **15**, 1593 (2023) <https://doi.org/10.3390/pharmaceutics15061593>.
- [39] Nagaich U, Gulati N. Nanostructured lipid carriers (NLC) based controlled release topical gel of clobetasol propionate: design and in vivo characterization. *Drug Deliv. and Transl. Res.*, **6**, 289–98 (2016) <https://doi.org/10.1007/s13346-016-0291-1>.
- [40] Youssef AAA, Thakkar R, Senapati S, Joshi PH, Dudhipala N, Majumdar S. Design of Topical Moxifloxacin Mucoadhesive Nanoemulsion for the Management of Ocular Bacterial Infections. *Pharmaceutics*, **14**, 1246 (2022) <https://doi.org/10.3390/pharmaceutics14061246>.
- [41] Youssef AAA, Dudhipala N, Majumdar S. Dual Drug Loaded Lipid Nanocarrier Formulations for Topical Ocular Applications. *IJN*, **Volume 17**, 2283–99 (2022) <https://doi.org/10.2147/IJN.S360740>.
- [42] Han H, Li S, Xu M, Zhong Y, Fan W, Xu J, Zhou T, Ji J, Ye J, Yao K. Polymer- and lipid-based nanocarriers for ocular drug delivery: Current status and future perspectives. *Advanced Drug Delivery Reviews*, **196**, 114770 (2023) <https://doi.org/10.1016/j.addr.2023.114770>.